Optimization of Superalloy Homogenization Cycles

Jared Smith, Alex Kaiser, Alex Post, John Schrader
Faculty Advisors: Professor David Johnson, Professor Michael Titus
Industrial Sponsor: Rob Christiansen

Individualized homogenization cycles were developed for HAYNES® 242® Ni-25Mo-8Cr, HAYNES® 25 Co-20Cr-15W-10Ni, and HASTELLOY® C-2000® Ni-23Cr-16Mo (wt.%) superalloys with the aim to reduce energy cost. Homogenization cycle dwell temperatures were determined from analysis of phase dissolution and solidus temperatures calculated in Thermo-Calc. Minimum hold times were determined from a simple analytical model. The homogenization cycle time for HAYNES® 25 was reduced by 55%. Further testing is necessary to validate proposed cycles for HAYNES® 242® and HASTELLOY® C-2000®, but the proposed cycles reduce cycle time by 4% and 9%, respectively.

This work is sponsored by Haynes International in Kokomo, IN

Project Background

Haynes International is a superalloy manufacturer that currently produces over 40 different nickel, cobalt, and iron based superalloys. Haynes International produces these alloys as shown in **Figure 1**.

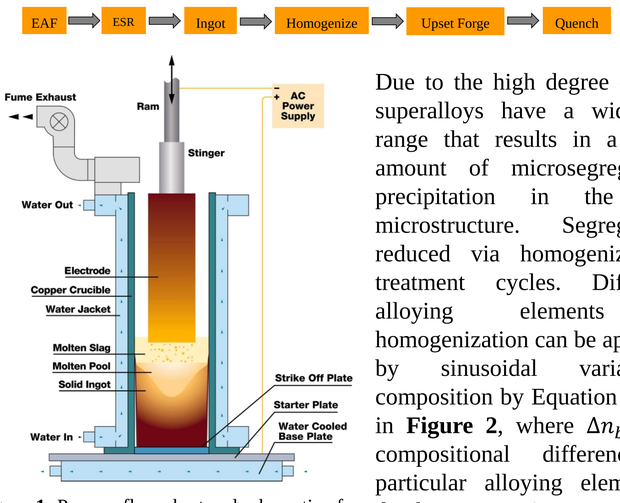

Figure 1: Process flow chart and schematic of electro slag remelt (ESR) process [1]

Due to the high degree of alloying, superalloys have a wide freezing range that results in a significant amount of microsegregation and precipitation in the dendritic microstructure. Segregation is reduced via homogenization heat treatment cycles. Diffusion of alloying elements during homogenization can be approximated by sinusoidal variations in composition by Equation 1 as shown in **Figure 2**, where Δn_b is half the compositional difference of a particular alloying element across dendrite arms, Δn_{bo} is half of the original compositional difference, t is time in seconds, and τ is the relaxation time, which is a function of dendrite arm spacing and the alloying diffusion coefficient, seen in **Equation 2**. [2]

$$\Delta n_b = \Delta n_{bo} e^{-t/\tau} \quad \text{(Equation 1)}$$

$$\tau = l^2/\pi^2 D \quad \text{(Equation 2)}$$

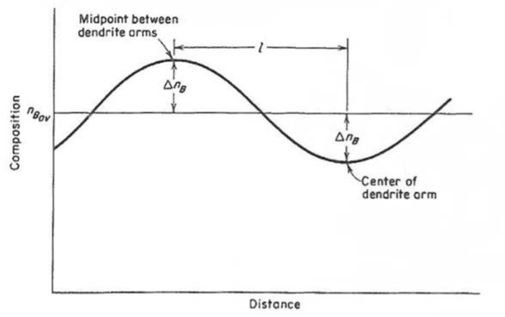

Figure 2: Graph showing the sinusoidal variation in composition of a diffusing element across a dendrite arm.

Experimental Procedure

Sample Preparation

ESR sections from three alloy compositions, HAYNES® 242® Ni-25Mo-8Cr, HAYNES® 25 Co-20Cr-15W-10Ni, and HASTELLOY® C-2000® Ni-23Cr-16Mo (wt.%), were obtained for metallurgical analysis as shown in **Figure 3**.

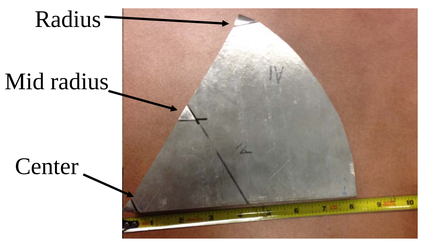

Figure 3: As received section from the end of the steady state region of an ESR ingot.

Method for Determining Proposed Homogenization Cycle

I) Measure secondary dendritic arm spacing in as-cast microstructure to calculate Δn_b from **Equation 1**.
II) Calculate Equilibrium Solidus temperature from Thermo-Calc.
III) Calculate Scheil solidus temperature from Thermo-Calc.
IV) Calculate phase solvus temperatures from equilibrium cooling plot in Thermo-Calc to determine homogenization heat treatment steps to avoid incipient melting, and measure Δn_{bo} from EDS.
V) Calculate $\Delta n_{b,standard}$ from **Equation 1** using diffusion coefficient found in literature for the most segregated element, SDAS, and Δn_{bo} from EDS on known standard homogenization cycle.
VI) Determine proposed homogenization cycle by using temperature steps found in equilibrium cooling plot and ramp to temperature between scheil solidus and equilibrium solidus temperatures in order to achieve $\Delta n_{b,proposed} \leq \Delta n_{b\_standrd}$ in less time.

Validation of Proposed Homogenization Cycles

The degree of remaining microsegregation can be determined by using a known phase diagram and by characterizing the precipitation behavior at different temperatures. The bisection method is used to find the minimum temperature difference between which precipitates do and do not form to find a theoretical residual compositional difference between standard and proposed homogenization cycles.

Results

I) Secondary Dendrite Arm Spacing

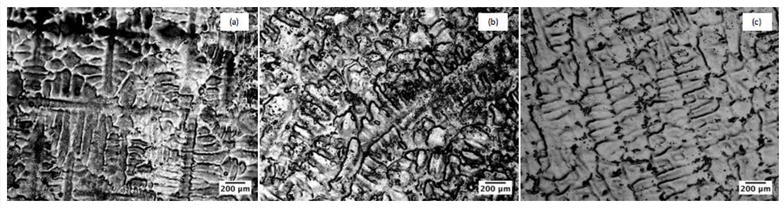

Figure 4: Optical micrographs taken at the mid radius of the ingots showing as-cast dendrites of HAYNES® 242® (a), HAYNES® 25 (b), and HASTELLOY® C-2000® (c).

Table I: *Dendrite Arm Spacings Measured at Ingot Mid-Radius*

Alloy	Primary DAS (with 95% confidence interval) in µm	Secondary DAS (with 95% confidence interval) in µm
HAYNES® 242®	687 ± 75	115 ± 8.0
HAYNES® 25	697 ± 69	122 ± 14
HASTELLOY® C-2000®	745 ± 23	106 ± 10

II & III) Equilibrium and Scheil Solidus

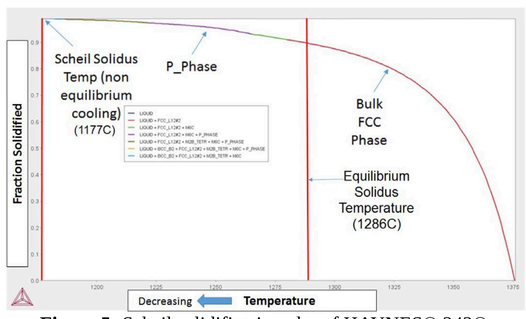

Figure 5: Scheil solidification plot of HAYNES® 242®

IV) Secondary Phase Solvus

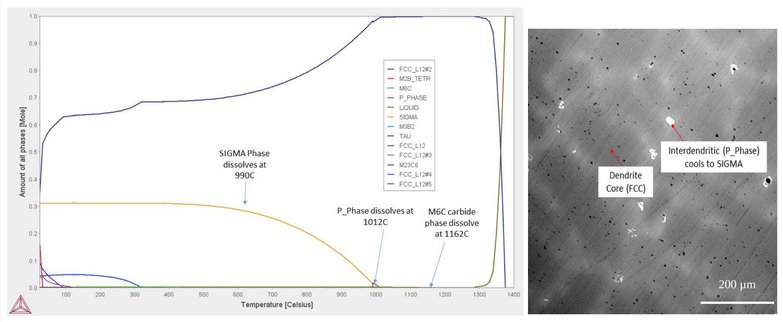

Figure 6: Equilibrium cooling plot and as-cast SEM microstructure of HAYNES® 242® showing Mo rich σ phase precipitation in Ni FCC matrix and phase solvus temperatures. Compositional difference across dendrite arms measured as Δ25.9 wt% Mo. Equilibrium and Scheil solidus temperatures were calculated as 1286°C and 1177°C, respectively.

V) & IV) Determination of Proposed Homogenization Cycle

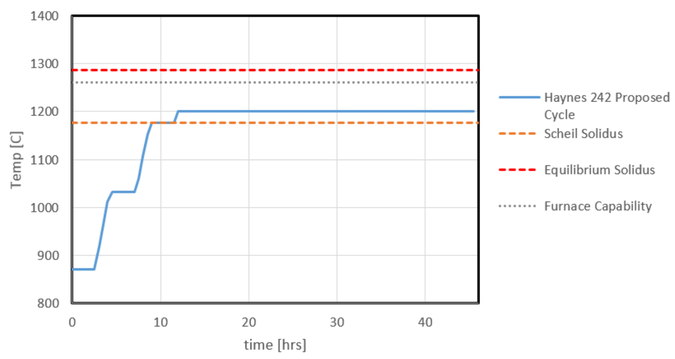

Figure 7: Diagram showing homogenization heat treatment steps of proposed homogenization cycle for HAYNES® 242®.

Proposed Homogenization Cycles

Table II: *Proposed Homogenization Heat Treatment Cycles*

Alloys	Proposed Homogenization Cycle	Justification for each step	Total Cycle Times
HAYNES® 242®	**Step 1**: 1032°C/3h **Step 2**: 1177°C /3h **Step 3**: 1200°C/33h/WQ	**Step 1**: Dissolve P and σ phases **Step 2**: Dissolve carbide phase **Step 3**: Minimize cycle time	Standard: 47.2h *Proposed: 45.5h*
HAYNES® 25	**Step 1:** 1175°C/3h **Step 2:** 1250°C/23h/WQ	**Step 1:** Dissolve R phase **Step 2:** Minimize cycle time	Extended: 87.3h *Proposed: 39.0h*
HASTELLOY® C-2000®	**Step 1:** 1070°C/3h. **Step 2:** 1260°C/21h/WQ	**Step 1:** Dissolve P and σ phases **Step 2:** Minimize cycle time	Standard: 34.2h *Proposed: 31.2h*

Discussion

Microstructural Comparison of Haynes Standard to Proposed Cycle

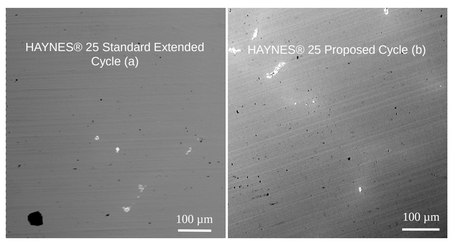

Figure 8: SEM images of HAYNES® 25 after the standard homogenization extended cycle (a) and our proposed homogenization cycle (b) showing 0.16 and 0.39 area percent of secondary phase precipitates, respectively.

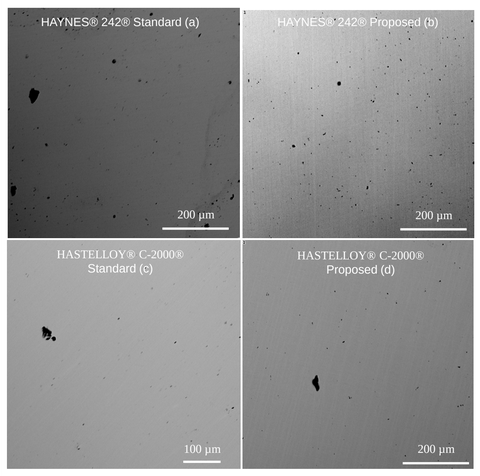

Figure 9: SEM images of HAYNES® 242® after the standard homogenization cycle (a) and our proposed homogenization cycle (b) and HASTELLOY® C-2000® after the standard homogenization cycle (c) and our proposed homogenization cycle (d) all showing zero area percent of secondary phase precipitates.

HAYNES® 25 continued to show secondary phase precipitation even after extremely long homogenization hold times. Our proposed cycle was further tested by upset forging prior to the quench. After upset forging, the drop in temperature increased the secondary phase precipitate area percent to 1.6% in both Haynes extended cycle and the cycle proposed in this study. Since there was no statistical difference after upset forging, our proposed cycle was deemed effective reducing the total homogenization cycle time for this alloy by 55%, a 48 hr reduction.

HAYNES® 242® and HASTELLOY® C-2000® showed no remaining secondary phase precipitation after either Haynes standard homogenization cycles or the cycles proposed in this study as shown in the SEM micrographs of **Figure 9**. To further validate our proposed homogenization heat treatment cycle, a series of validation heat treatments were performed on both alloys. Temperatures for these treatments were selected from isopleths calculated in Thermo-Calc. The isopleths were calculated as a function of Mo concentration because it was the most segregated element in the two alloys.

Compositional Validation of Homogenization Cycles

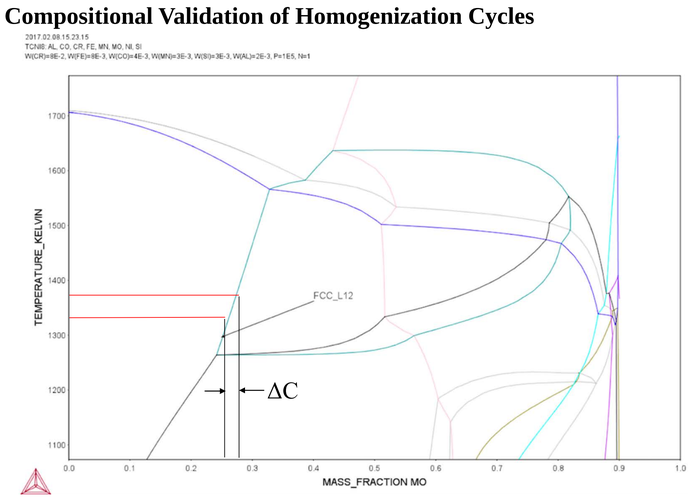

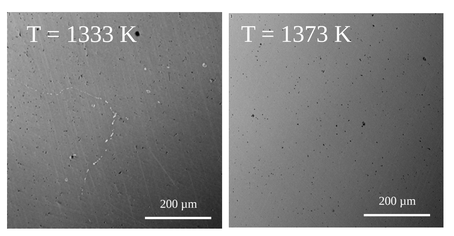

Figure 10: (top) Isopleth of HAYNES® 242®, (bottom) Resulting microstructure after validation HT at 1333 K and 1373 K showing a residual compositional gradient within ± 0.4 wt % Mo.

Recommendations

The standard homogenization cycle used for HAYNES® 25 could be replaced by our cycle due to identical microstructure after forging.

The standard homogenization cycles used for HAYNES® 242® and HASTELLOY® C-2000® could be replaced with our proposed cycles if further testing were to validate similar residual compositional gradients.

References

[1] Innovative Research, LLC, http://inresllc.com/products/meltflow/meltflow-esr.html
[2] Abbaschian, R., and Reed-Hill, R.E., "Solidification of Metals," Ch. 14, *Physical Metallurgy Principles - SI Version*, pp. 408-462.

MSE 430-440: Materials Processing and Design